Collapse from the Top: Brushes of Poly(*N*-isopropylacrylamide) in Co-nonsolvent Mixtures

Qi Chen,[a] E. Stefan Kooij,[b] Xiaofeng Sui,[a b] Clemens J. Padberg,[a] Mark A. Hempenius[a], Peter M. Schön,[a] and G. Julius Vancso[*a]

[a] *Department of Materials Science and Technology of Polymers, University of Twente, MESA+ Institute for Nanotechnology, P.O. Box 217, 7500 AE Enschede, The Netherland.*
**Correspondence to: Prof. G. Julius Vancso, Fax: +31 (0)53 489 3823;Tel: +31-53-4892967, E-mail: g.j.vancso@utwente.nl*
[b] *Physics of Interfaces and Nanomaterials, MESA+ Institute for Nanotechnology, University of Twente, P.O. Box 217, 7500AE Enschede, The Netherlands.*

Supporting Information

Analysis of ellipsometry spectra

Silicon substrate

The ellipsometry spectra, i.e. Ψ and Δ as a function of wavelength (275-827 nm) were analyzed employing the package CompleteEASE (Woollam), using bulk dielectric functions for silicon, silicon dioxide and water. The substrate was in all cases considered to consist of silicon with a silicon dioxide film. In Fig. S1 a typical ellipsometry measurement for the bare silicon substrate (coated with a natural oxide layer of 1.7nm, as deduced from the fit) obtained at an angle of incidence θ=65º, prior to deposition of the PNIPAM brush. The characteristic features for silicon are clearly observed: A peak in Ψ near 365nm and steps in the variation of Δ near 290nm and 375nm.

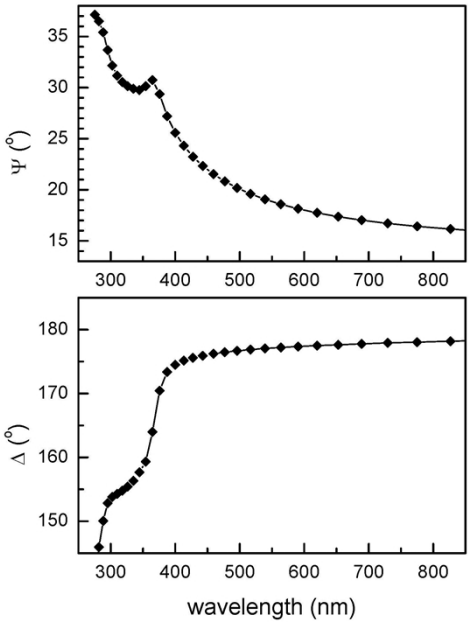

Figure S1 Ellipsometry spectra of a bare silicon substrate, with a 1.7nm natural oxide film; the solid line represents a fit to the data. The angle of incidence amounts to θ=65º.

Cauchy modeling

For all spectra, the analysis of the PNIPAM brushes was performed on the basis of the Cauchy model. Below we will specify how the Cauchy description was applied. For dry films, a homogeneous layer provides a good description, while PNIPAM brushes in contact with a liquid (water/methanol, or pure water) exhibited a density gradient across the film thickness. The refractive index of the thin PNIPAM film was parameterized by using the Cauchy dispersion relation which is given by

$$\lambda = A + \frac{B}{\lambda^2} + \frac{C}{\lambda^4}$$

in which the wavelength λ is in microns. The quantities *A*, *B* and *C* represent fit parameters. In the analysis of our experimental spectra, we set $C = 0$ since it does not yield improved fit results and often gives rise to large correlations with other fit parameter. Furthermore, in all cases we assumed the PNIPAM to be fully transparent, i.e. the refractive index is a real quantity (the imaginary part describing optical absorption is neglected).

Dry PNIPAM brush films

The optical response of dry films prior to immersion in the solution could be properly described (Fig. S2) using a homogeneous film of which the refractive index was represented by a single non-graded Cauchy relation. The ambient was air, for which a refractive index $n = 1$ was taken in the model. For the thicker films (HD, and MD) we used the film thickness *d* and the two Cauchy parameters *A* and *B* as fitting parameters. The resulting fit parameters are summarized in Table 1; the corresponding wavelength dependence of the refractive index corresponding to these parameters is shown in Fig. S3.

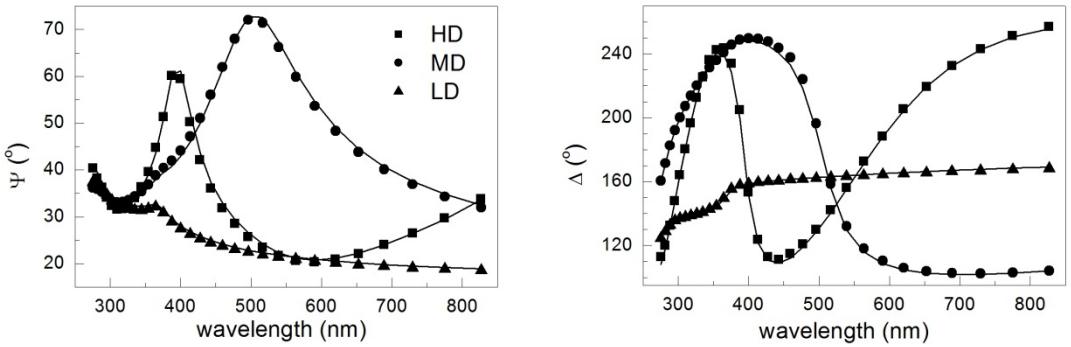

Figure S2. Experimental ellipsometry spectra (symbols) and fit results (solid lines) for the dry PNIPAM films using the model as described in the text.

For the thinnest film (LD), it proved difficult to separate the refractive index contribution from that of the thickness. For these low film thicknesses, optical reflection measurements are only sensitive to the product $n \cdot d$ of the refractive index and the thickness. Setting all of them as fit parameters results in undefined fits with a high correlation between *A* and *d*. As such, for the low grafting density brush we used an average of the Cauchy parameters of the thicker films and only fitted the thickness. The resulting value is included in Table 1.

Table 1. Fit parameters for the optical modeling of dry PNIPAM films using a single homogeneous Cauchy layer. The values between brackets () were inserted into the model, but have not been varied in the fitting procedure.

	HD	MD	LD
d (nm)	245.5	103.1	8.73
A (μm^2)	1.453	1.467	(1.46)
B (μm^2)	0.00495	0.00621	(0.0055)

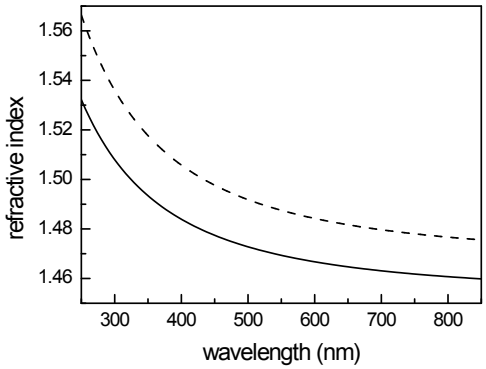

Figure S3. Refractive index of the HD and MD PNIPAM brushes (solid and dashed lines, respectively) as a function of wavelength.

PNIPAM brush in pure water

When the PNIPAM brush films are immersed into pure water, they exhibit substantial swelling. Correspondingly, their optical properties become very much diluted. This makes it relatively difficult to obtain accurate fit results. As shown in the spectra in Fig. S4 all spectra clearly contain features reminiscent of the substrate. Most pronounced is the peak near 365nm in Ψ and the shoulder step-like increase at 300nm. Nevertheless, the slight variations, including the oscillations discerned most clearly in the spectra of the HD films, enabled a reasonable fitting.

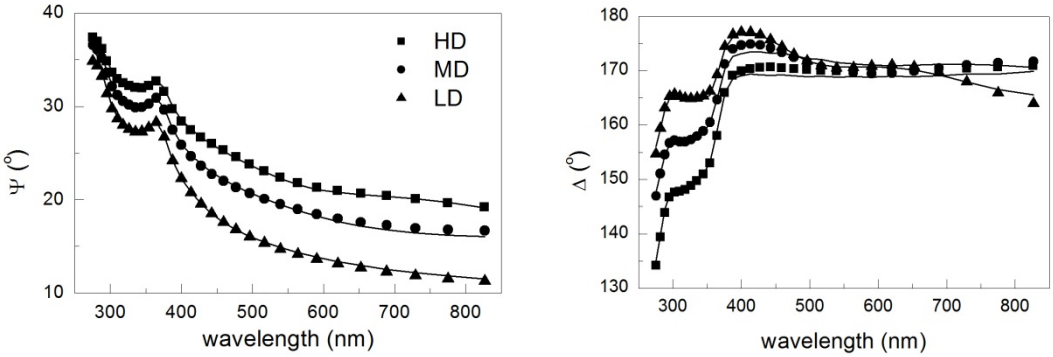

Figure S4. Experimental ellipsometry spectra (symbols) and fit results (solid lines) for the PNIPAM films immersed in pure water, using the model as described in the text.

To obtain acceptable fits, it was necessary to use a more complicated model in the analysis [1]. For the high and medium grafting density films, a two-layer model was used to describe the optical response of the brush film. In this two-layer model, a dense film at the substrate side of the film was modeled with a thickness d_1 and Cauchy parameters A_1 and B_1. The outer part of the film (for the low grafting density the entire film) was modeled using a graded Cauchy film, with parameters d_2, A_2 and B_2 and an exponential grading of the A_2 parameter. The total film thickness d is the sum of d_1 and d_2.

The exponential grading of the parameter $A_2(z)$ as used in the analysis can be represented by

$$A_2(z) = A_2\left(1 - \frac{\delta A}{2} + \delta A \cdot z^t\right)$$

with z the relative position within the film (the substrate is at $z = 0$; $z = 1$ corresponds to the outer side of the film) and t and δA are fitting parameters. A negative value of the grading parameter δA corresponds to a decreasing density (refractive index) for larger distances from the substrate.

As shown in Fig. S4, the overall fit results are fairly good. All features in the spectra are reproduced. The fit parameters summarized in Table 2 show that approximately 8-10% of the film is described by a homogeneous Cauchy dispersion. The rest of the film (referred to as the second layer) shows a decline of the refractive index with decreasing distance from the substrate. The decline as shown in Fig. S5 (right) is from large values at the interface between layer 1 and 2, to values very close to that of water (n = 1.33 at 600 nm). As already described above, the outer parts of the layer are diluted to such an extent that only a few PNIPAM brush-ends are surrounded by a large amount of water. The difficulty in quantitatively analyzing the LD films is obvious from the result in Fig. S5 (right); owing to the correlation between thickness and refractive index, the gradient within the LD films becomes rather steep. Verifying the correlation coefficients obtained in fitting the ellipsometry spectra indeed confirms the large errors in the steepness of the gradient.

Table 2. Fit parameters for the optical modelling of PNIPAM films immersed in pure water, using a two-layer model as described in the text. The value between brackets () were inserted into the model, but have not been varied in the fitting procedure.

	HD	MD	LD
d_{total} (nm)	901.5	567.4	35.5
d_1 (nm)	90.0	52.4	0.0
A_1 (μm^2)	1.416	1.389	-
B_1 (μm^2)	0.00529	0.00322	-
d_2 (nm)	811.5	515.0	35.5
A_2 (μm^2)	1.396	1.360	1.429
B_2 (μm^2)	0.00414	0.00467	(0.0)
δA (%)	-10.3	-5.79	-14.6
t	0.171	0.327	(0.3)

Similar to the difficulties with the analysis of the dry, low grafting density samples, here there is also a problem in obtaining reliable fit results. The additional dense layer at the substrate is not required. Also, the exponent is set fixed. Using these values a relatively large gradient is observed, which may be related to the omission of a dense layer at the substrate side of the film.

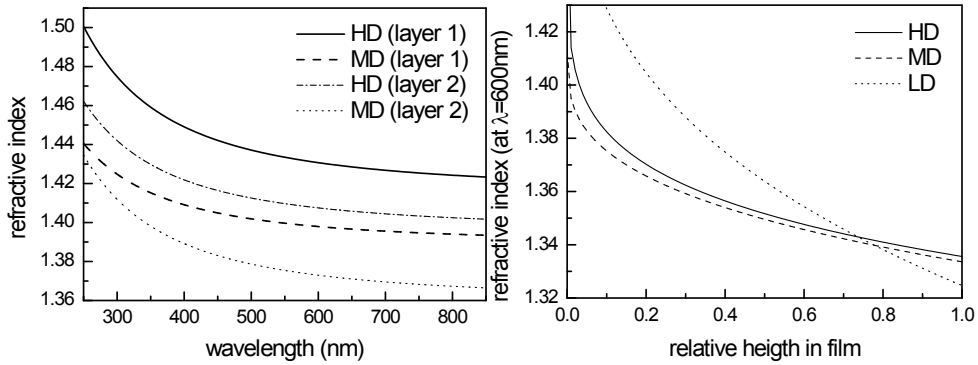

Figure S5. (left) Refractive index values as described by the Cauchy parameters in Table 2 for both layers within the modeled HD and MD films. (right) Variation of the refractive index at a

wavelength of 600nm for the second layer in three different films, as a function of the relative height z within the film. The substrate corresponds to z = 0; the film-liquid interface is at z = 1.

PNIPAM brush in methanol-water

Immersion of the PNIPAM brushes into a methanol-water mixture gives rise to a markedly different optical response as compared to that in water (Fig. S6). We attribute these changes to considerable de-swelling of the PNIPAM brush in the co-nonsolvent mixture. To enable accurate analysis, we consider the optical properties of the liquid to be equal to that the refractive index of water. Methanol has a very similar refractive index; we assume that the optical characteristics of the mixture can also be represented by those of pure water.

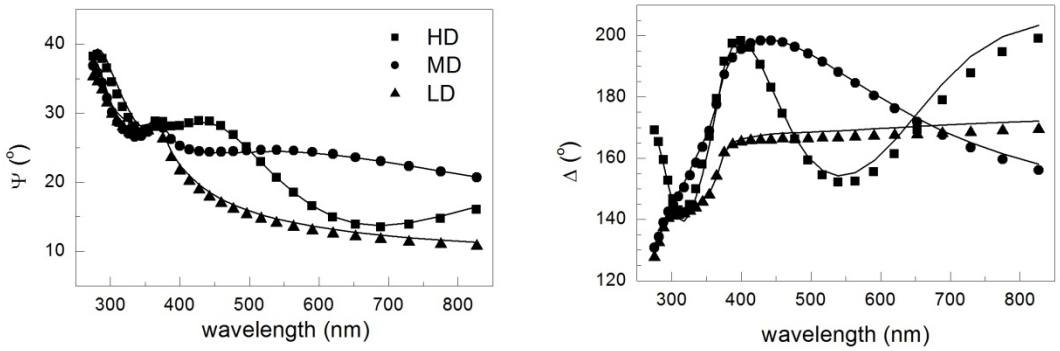

Figure S6. Experimental ellipsometry spectra (symbols) and fit results (solid lines) for the PNIPAM films immersed in methanol-water mixture, using the model as described in the text.

We started the analysis based on the model for PNIPAM brushes in water [1]. Moreover, considering the sequence in which we immersed the samples (first in water, followed by transfer to mixed co-nonsolvent), we assume that the dense layer on the substrate side of the film remains unchanged. We only take into account changes in the outer diluted layer, and more specifically attempt to model the collapse of the outer layer. Several models were considered which give similar results; a major challenge is to keep the number of fitting parameters limited. Below we describe the procedure as used for the results presented in this manuscript.

To accommodate the partial collapse, we assumed a symmetric profile of the refractive index parameter of the A described by

$$A_2(z) = A_2^{'} + A_2^{''}(z - 0.5)^n$$

where $A_2^{'}$ and $A_2^{''}$ are fitting parameters and z represents the relative surface-normal position within the film, as we did for the PNIPAM brushes in water. The exponent n was chosen to be an even integer, which best fits the data; for the HD sample n=6 and for the MD sample n=2. For the LD samples it was not possible to derive any information on the gradient. For these low grafting densities, the entire film is modeled using a simple homogeneous Cauchy model without any grading, i.e. n=0.

The resulting spectra obtained by fitting are shown in Fig. S6 by the solid lines. For the HD and MD samples, we obtained the best results using $A_2(z)$= 1.389 + 1.69 (z-0.5)^6 and $A_2(z)$= 1.374 + 0.06 (z-0.5)^2, respectively. The resulting thickness values are summarized in Table 3.

Table 3. Thickness values as deduced from the optical modeling of PNIPAM films immersed in methanol-water mixtures, using the model described in the text.

	HD	MD	LD
d_{total} (nm)	435.6	209.1	19.7
d_1 (nm)	90.0	52.4	-
d_2 (nm)	345.6	156.7	19.7

Comparison between temperature-induced and co-nonsolvent collapse

Finally, in the analysis the question arose whether the spectra of collapsed PNIPAM brushes in the co-nonsolvent mixture compares to any of the spectra obtained during the temperature-induced collapse as presented in our previous publication [1].

In the supporting information of that paper, we included a figure similar to that below in Fig. S7 in which we presented the temperature-dependent ellipsometry parameters Ψ and Δ for the different brushes samples at specific energies. For the spectra in co-nonsolvent, these values can also be extracted; the dashed lines in Fig. S7 represent the corresponding Ψ and Δ values.

From this comparison it is obvious that indeed the spectra in water-methanol mixtures do not agree with any of the spectra measured during the *T*-induced collapse. Thus in turn confirms the fact that a different model must be used to describe the partly collapsed layers in the co-nonsolvent mixture.

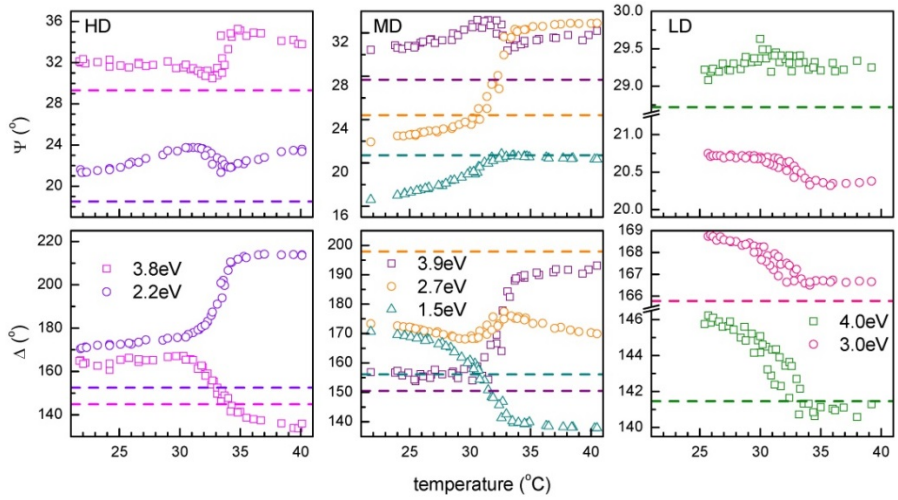

Figure S7. Comparison between ellipsometric quantities Ψ and Δ for the temperature-induced collapse transition at different photon energies (symbols) and the corresponding values for spectra of partly collapsed layers in water-methanol mixtures.

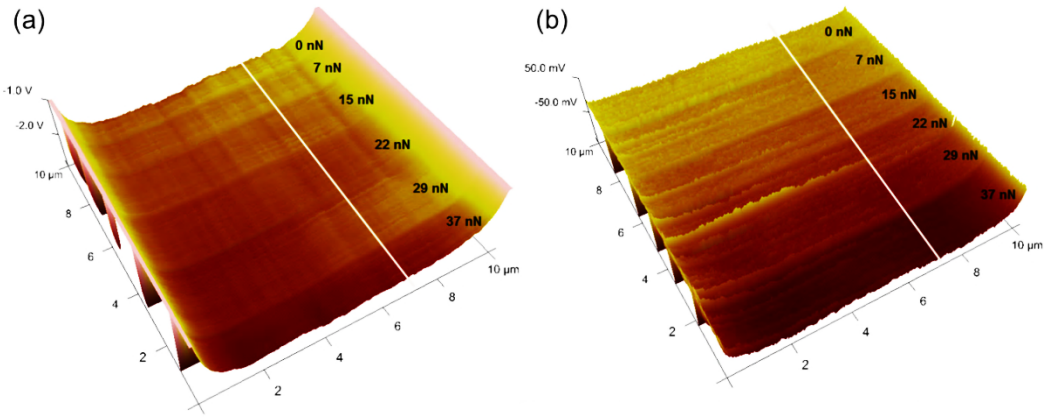

Figure S8. Friction images of the MD PNIPAM sample (a) in water/methanol 50% v/v and (b) in pure water; the applied load is increased from top to bottom as indicated. Note that the vertical scale of both images is not the same, but varies by a factor of 20.

Torsional sensitivity and spring constant calibration of the colloidal probe

As outlined in the review by Munz [2] on calibration in friction force microscopy using an atomic force microscope, there are several ways to transfer the actually measured signal, i.e. the photodetector voltage, to the actual lateral force acting on the cantilever, or any probing particle at the end of it. The force leads to a displacement Δx at the position where the cantilever (or a colloidal particle attached to it) interacts with the surface, which in turn gives rise to a torsional deformation ϕ of the cantilever. In the end, the deformation of the cantilever leads to a lateral deflection signal at the photodetector, which is expressed in a voltage. Below we describe the cantilever and colloidal probe used in our experiments, including a specification of relevant details on the geometry of the cantilever, and the relevant sensitivities and force constants.

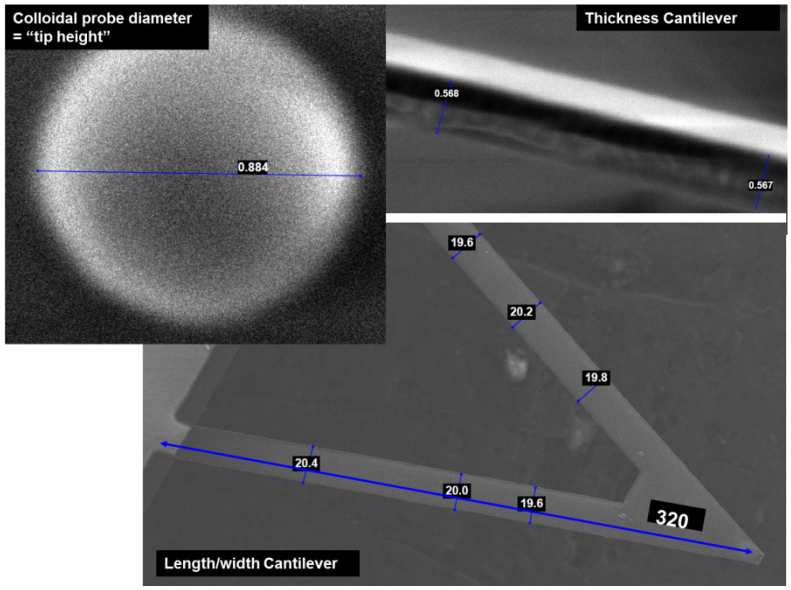

Figure S9. SEM images of cantilever and colloidal probe with measured lengths in µm.

Average dimensions from SEM pictures

w = 20 µm (width)

t = 0.57 µm (cantilever thickness)

c = 320 µm (cantilever *leg* length)

l = 300 µm (cantilever *projected* length, side view)

h = 1.18 µm (diameter colloidal probe + ½ t)

Lateral deflection sensitivity in nm/V

For the calculation of the lateral deflection sensitivity based on the vertical deflection sensitivity the following formula from Tocha et al. [3] was used:

$$S_L = \frac{P}{aRl} h S_N$$

with

P = 2.5 ± 0.5 (proportionality factor for V shaped cantilevers)

a = 4.1 (amplification factor in AFM system, i.e. for Multimode Nanoscope (Bruker))

R= 0.5 (correction factor for V-shaped cantilever)

l = 300 μm (cantilever projected length)

h = 1.18 μm (diameter colloidal probe + ½ t)

S_N = 73.3 nm/V (vertical deflection sensitivity)

Inserting these numbers, we obtain the lateral deflection sensitivity:

S_L = 0.34 nm/V

Torsional sensitivity

The torsional sensitivity [4] was derived from the assumption that lateral displacement of the colloidal probe at the contact area translates into a corresponding torque of the cantilever, according to the illustration below:

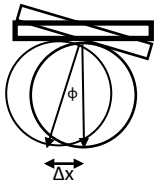

Figure S10. Schematic front view on colloidal probe to illustrate derivation of torsional spring constant from lateral displacement.

Considering the geometry of the colloidal probe-cantilever systems, trigoniometric relations yield the torsional sensitivity. Using

$$\tan \phi = \Delta x / h$$

with

ϕ = torque in rad

Δx = displacement in lateral direction

h = 1.18 μm (diameter colloidal probe + ½t, with t the cantilever thickness)

we obtain the torsional sensitivity of the cantilever:

S_ϕ = 0.29 mrad/V (or 3.45 x 10^3 V/rad)

The lateral spring constant was calculated according to the method of Sader et al. [5]

k_ϕ = 5.24 x 10^{-10} Nm·rad^{-1}

k_L = 380 N/m

References

[1] E.S. Kooij, X. Sui, M. A. Hempenius, H. J. W. Zandvliet and G. J. Vancso, J. Phys. Chem. B **116** (2012) 9261-9268

[2] M. Munz, J. Phys. D: Appl. Phys. **43** (2010) 063001

[3] E. Tocha, H. Schönherr and G. J. Vancso, Langmuir **22**, 2006, 2340-2350

[4] T. Pettersson, N. Nordgren, M.W. Rutland, and A. Feiler, Rev. Sci. Instrum. **78** (2007) 093702

[5] J.E. Sader, Rev. Sci. Instrum. **74** (2003) 2438-2443